

# Magnetic field sensitivity of the photoelectrically read nitrogen-vacancy centers in diamond

Cite as: Appl. Phys. Lett. **120**, 162402 (2022); <https://doi.org/10.1063/5.0079667>

Submitted: 23 November 2021 • Accepted: 22 February 2022 • Published Online: 19 April 2022

Published open access through an agreement with Universiteit Hasselt

 Jaroslav Hruby,  Michal Gulka,  Massimo Mongillo, et al.



View Online



Export Citation



CrossMark

## ARTICLES YOU MAY BE INTERESTED IN

[A perspective on electrical generation of spin current for magnetic random access memories](#)  
Applied Physics Letters **120**, 160502 (2022); <https://doi.org/10.1063/5.0084551>

[van der Waals epitaxy of 2D h-AIN on TMDs by atomic layer deposition at 250 °C](#)  
Applied Physics Letters **120**, 162102 (2022); <https://doi.org/10.1063/5.0083809>

[Excitation of tunable plasmons in silicon using microwave transmission through a metallic aperture](#)  
Applied Physics Letters **120**, 162103 (2022); <https://doi.org/10.1063/5.0080262>

Lock-in Amplifiers  
up to 600 MHz



Zurich  
Instruments



# Magnetic field sensitivity of the photoelectrically read nitrogen-vacancy centers in diamond

Cite as: Appl. Phys. Lett. **120**, 162402 (2022); doi: 10.1063/5.0079667

Submitted: 23 November 2021 · Accepted: 22 February 2022 ·

Published Online: 19 April 2022



View Online



Export Citation



CrossMark

Jaroslav Hruby,<sup>1,2</sup> Michal Gulka,<sup>1,3</sup> Massimo Mongillo,<sup>4</sup> Iuliana P. Radu,<sup>4</sup> Michael V. Petrov,<sup>1,2</sup> Emilie Bourgeois,<sup>1,2</sup> and Milos Nesladek<sup>1,2,a)</sup>

## AFFILIATIONS

<sup>1</sup>Institute for Materials Research (IMO), Hasselt University, Wetenschapspark 1, B-3590 Diepenbeek, Belgium

<sup>2</sup>IMOMEC Division, IMEC, Wetenschapspark 1, B-3590 Diepenbeek, Belgium

<sup>3</sup>Institute of Organic Chemistry and Biochemistry, Czech Academy of Sciences, 166 10 Prague, Czech Republic

<sup>4</sup>IMEC, Kapeldreef 75, Leuven B-3001, Belgium

<sup>a)</sup> Author to whom correspondence should be addressed: [milos.nesladek@uhasselt.be](mailto:milos.nesladek@uhasselt.be)

## ABSTRACT

In this work, we report on the sensitivity of photo-electrical detection of magnetic resonances (PDMR) for magnetometry measurement using low density nitrogen vacancy (NV) ensembles in CVD-grown diamond. We demonstrate that the selection of the laser excitation wavelength is of importance for achieving optimal magnetic field sensitivity. The PDMR sensitivity obtained using a yellow-green (561 nm) laser surpasses the performances of a green laser (532 nm), by suppressing the photoionization of defects other than NV centers (such as P1 centers). It consequently allows to carry out the PDMR measurements at lower laser powers with increased magnetic resonance contrast. Noticeably for both the green and the yellow-green illuminations, PDMR leads to an improved sensitivity to magnetic fields in the selected conditions compared to optically detected magnetic resonance.

© 2022 Author(s). All article content, except where otherwise noted, is licensed under a Creative Commons Attribution (CC BY) license (<http://creativecommons.org/licenses/by/4.0/>). <https://doi.org/10.1063/5.0079667>

Magnetic field sensors are widely used in applications, including consumer electronics and space probes. Their working principles are mainly based on classical electro-magnetism or semiconducting principles, such as the Hall effect or giant magnetoresistance (GMR). A new generation of magnetometers that works on quantum mechanical principles, such as superconducting quantum interference devices (SQUIDS) and vapor phase magnetometers,<sup>1,2</sup> have been developed in parallel. One of the possible magnetometer configurations, which recently triggered significant interest, is based on the nitrogen vacancy (NV) color center in diamond.<sup>3-5</sup> The NV spin sensor can detect the magnetic field through the detection of the Zeeman split between the  $m_s = -1$  and  $m_s = +1$  spin sublevels or through phase accumulation when  $m_s = 0$  and  $m_s = (-1)$  are in a superposition state. Compared to other devices, the NV spins offer advantages in terms of vector field magnetometry, wide dynamic range, long term stability, and room-temperature operation.<sup>3,4</sup> So far, optically detected magnetic resonance (ODMR) NV magnetometers, based on the detection of the photoluminescence emitted by NV centers under excitation [see Fig. 1(a)], have been studied.<sup>5-7</sup> Sensitivities ranging from typically  $1 \text{ nT/Hz}^{1/2}$  to below  $1 \text{ pT/Hz}^{1/2}$ ,<sup>3</sup> depending on the experimental configuration and

the type of detection protocols used, have been reached. However, the main challenge for practical applications of such devices remains their miniaturization and integration into compact devices.<sup>7</sup>

Alternatively, the NV spin state can be read using the recently established Photoelectric Detection of Magnetic Resonances (PDMR).<sup>8-13</sup> PDMR makes the use of the spin-state-dependent photocurrent resulting from NV centers two-photon ionization [Fig. 1(a)] and might provide a pathway to compact sensors integrated with electronics. The essential parameter to evaluate the performance of such detectors is the detection sensitivity. In this work, we evaluate the shot noise limit of the magnetic field sensitivity of a continuous-wave (CW) PDMR-read device and compare it with CW ODMR readout executed in parallel on the same sample. The highest sensitivities using NV centers have been achieved so far by employing the ODMR technique in dense NV ensembles (concentrations in the range of 1 ppm or higher).<sup>6</sup>

Nevertheless, there is also a range of applications using magnetometers with single NV centers with a typical CW sensitivity of  $\sim 1 \mu\text{T/Hz}^{1/2}$  per NV.<sup>14</sup> For pulsed measurements, the sensitivity of  $\sim 10 \mu\text{T/Hz}^{1/2}$  has been reached using nanopillars for light detection.<sup>15</sup> The single NV center configurations is also used, for example, in scanning

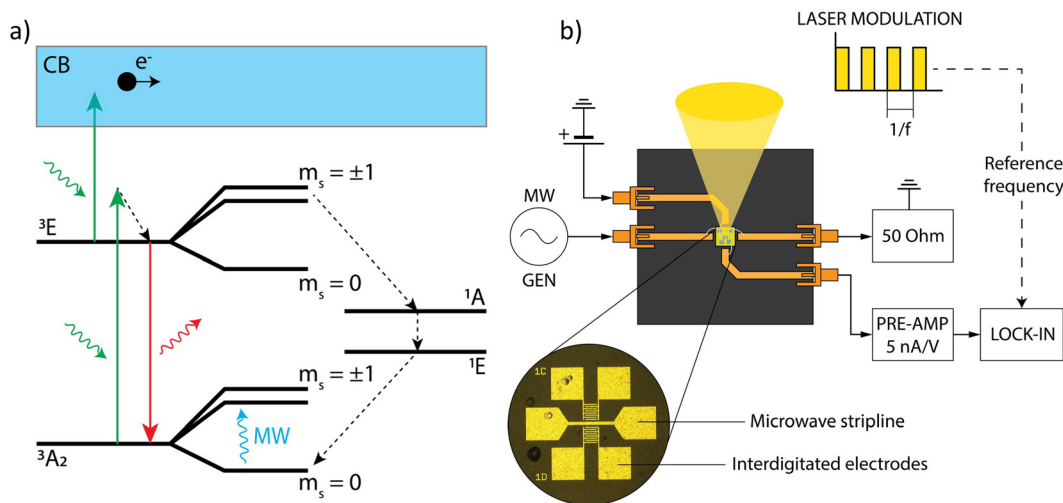


**FIG. 1.** (a) Energy level diagram of the negatively charged NV center, showing transitions responsible for ODMR and PDMR detection. The green arrows represent the NV two-photon excitation from the NV triplet ground state ( ${}^3A_2$ ) to the triplet excited state ( ${}^3E$ ) and subsequently from the  ${}^3E$  state to the conduction band (CB) resulting in the generation of a free electron ( $e^-$ ) contributing to the photoelectric signal. Alternatively, from the excited state, the electron can decay either radiatively emitting a visible photon (red arrow) or non-radiatively, through a spin-dependent transition to a singlet metastable state ( ${}^1E$  ground state and  ${}^1A$  excited state). The Zeeman splitting frequency is proportional to the applied magnetic field  $\Delta\nu = 2\gamma_{NV}B_z$ , where  $\Delta\nu$  is frequency splitting,  $\gamma_{NV}$  is the gyromagnetic ratio, and  $B_z$  is magnetic field applied along the NV axis. (b) Schematic of the PDMR chip used for experiments and the acquisition setup layout.

diamond magnetometry to map the magnetic field at nanoscale. Low-density ensembles with isolated NV centers spread in a 2D plane across the diamond surface can alternatively provide a high spatial resolution and mapping of the magnetic field in wide-field magnetometry configuration, relevant for instance for biological sensing.<sup>15</sup> For this reason, we concentrate our work on low-density NV ensembles. Additionally, in such a study, the complex spin interactions present in high-density ensemble systems can be omitted allowing a better comparison of electrical and optical detection sensitivity.

CW ODMR and PDMR measurements were performed under yellow-green (56) and green (532 nm) laser excitations. The selection of the excitation wavelength is important due to the presence of optoelectrically active defects other than NV centers in diamond crystals, in particular P1 centers (single substitutional nitrogen centers— $N_S$ ). These defects can be photoionized and, thus, contribute to the photoelectric signal, limiting the PDMR contrast.<sup>8–10,12,16</sup> We show that using yellow-green light, the PDMR contrast can be substantially enhanced compared to green illumination, leading also to a tenfold sensitivity improvement when compared to ODMR measured simultaneously on the same CVD diamond sample. The PDMR technique is of interest for the development of sensitive magnetometers capable of miniaturization and integration with electronics.

The PDMR and ODMR measurements were carried out using a custom-built microscope that allows simultaneous optical and electrical detection of magnetic resonances.<sup>8–10,12,16</sup> A green (532 nm) or a yellow-green (561 nm) gem laser from Laser Quantum was pulsed at a low frequency (131 Hz) using acousto-optic modulators. The laser-pulsing frequency was used as a reference for lock-in readout of the photocurrent. The laser beams were focused on the diamond sample using an air objective (40 $\times$ , numerical aperture of 0.95). The photoluminescence (PL) emitted by the diamond under excitation was filtered using 650 and 665 nm cutoff long-pass filters and detected in confocal mode using

an avalanche photodiode (APD). For the experiments, we used a diamond layer epitaxially grown by plasma-enhanced chemical vapor deposition (PDS-17 reactor from ASTeX) on top of a single-crystal high-pressure high-temperature [100] lb diamond. The sample has been grown from  $CH_4/H_2$  mixture using 99.9995  $CH_4$  source further purified using a MonoTorr filter, reducing additionally the background impurity content by three orders of magnitude.  $CH_4$  contained natural abundance of  ${}^{13}C$ . The thickness of the layer was  $\sim 22 \mu m$ . The residual nitrogen in the growth chamber led to the formation of NV centers with the concentration of  $\sim 10$  ppb (corresponding to  $\sim 200$  NV centers in the optical confocal volume) as estimated from PL intensity compared to a reference sample with known NV concentration. The grown diamond sample was acid-cleaned in fuming  $H_2SO_4$  with  $KNO_3$  and rinsed in de-ionized water. The NV electron spin coherence was measured showing  $T_2 = 2 \mu s$  and  $T_2^* = 500$  ns. It was equipped with interdigitated contacts (5  $\mu m$  gap) for photocurrent detection and with a microwave (MW) strip line for application of the MW field required for NV spin manipulations. Contacts and strip-lines were prepared by means of optical lithography using sputtering deposition and consisted of a 20 nm layer of titanium covered with a 100 nm layer of aluminum. The electrodes and the MW strip line were wire-bonded to the printed circuit board tracks [see Fig. 1(b)]. The proximity of the strip line to the measured NV ensembles ( $\sim$  ten of  $\mu m$ ) allows using low MW powers (i.e., lower than 100 mW), limiting, thus, the sample heating. A bias electric field ( $\sim 3 \times 10^4 V cm^{-1}$ ) was applied between the electrodes, and the collected photocurrent was pre-amplified (with a gain of  $2 \times 10^8 VA^{-1}$ ) using a Stanford Research SR570 pre-amplifier and detected using a lock-in amplifier (Stanford Research SR850). The bias electric field was applied for both ODMR and PDMR measurements, as the two methods were used simultaneously.

To acquire the ODMR and PDMR spectra, the MW frequency was varied with the step size of 1–2 MHz (or 150 kHz for hyperfine

measurements). Typically, 100 sweeps were acquired per spectrum with the duration of a single sweep of about 55 s. The IV characteristics measurements were carried out by sweeping the bias voltage from 0 V to +25 V while detecting the DC with a picoammeter (Keithley 486).

To perform magnetometry measurements, the degenerated  $m_S = -1$  and  $m_S = +1$  spin sublevels of the NV centers ground state [see Fig. 1(a)] were first split by applying an external magnetic field using a permanent neodymium magnet. The resulting characteristic eight-peak ODMR and PDMR spectra are depicted in Figs. 2(a) and 2(b). We remark that the spin contrast, defined below, of the 8 measured peaks was not evenly distributed, even when trying to fine-tune the magnetic field orientation with a precision below  $1^\circ$ . This effect could be attributed either to non-even incorporation of NV centers along the 4 main crystallographic directions during the CVD diamond growth or potentially to a not fully homogeneous magnetic field from our microscopic strip line antenna. The highest ODMR and PDMR signal contrast ( $C$ ) were obtained for the resonance line at  $\sim 2849$  MHz, which was, thus, selected for further measurements. First, the hyperfine splitting induced by the adjacent  $^{14}\text{N}$  nuclear spin was measured both optically and electrically for comparison, using the same conditions [see Figs. 2(c) and 2(d)]. These measurements showed that PDMR can measure hyperfine spectra, similarly to ODMR. Although the laser focus is the same for both methods, the ODMR detection volume is determined by single photon confocal resolution ( $\sim 500$  nm), whereas the PDMR the signal is collected from a volume defined by the convolution of the 2-photon absorption volume

and the electric field profile from which the charge carriers are generated.<sup>8,16,23</sup> Further on, to reach a higher detection sensitivity, hyperfine lines can be used, as shown in Figs. 2(c) and 2(d).<sup>12</sup>

We define the measurement contrast as

$$C = (S_{\text{resonant}} - S_{\text{off-resonant}}) / S_{\text{off-resonant}}, \quad (1)$$

where  $S$  is the photoluminescence or photoelectric signal measured either at resonant or off-resonant MW frequency. From previous works,<sup>8,9,16</sup> we have found that P1 centers incorporated during the CVD growth reduce the measured PDMR spin contrast when using 532 nm green laser for the spin state readout and polarization. This is due to the fact that the measured current is increased by additional photocurrent generated from photoionization of P1 centers and other opto-electrically active defects.

For this reason, we compared two laser wavelengths (i.e., 532 and 561 nm). While the green laser photoionizes the P1 centers,<sup>17–20</sup> the P1 photoionization cross section is significantly reduced for yellow-green excitation.<sup>17,19</sup> Conversely, the cross sections for  $\text{NV}^-$  photoionization and for repumping of  $\text{NV}^0$  to the original  $\text{NV}^-$  charge state after the photoionization differ only slightly for the two used laser wavelengths.<sup>21,22</sup>

To characterize the photocurrent value, we have measured the current–voltage (I–V) characteristics for different laser powers for both used wavelengths. For these measurements, we did not apply any MW field. The resulting I–V curves are depicted in Figs. 3(a) and 3(b). It should be mentioned that the photogenerated current includes the electron current and the hole current produced by the repumping of

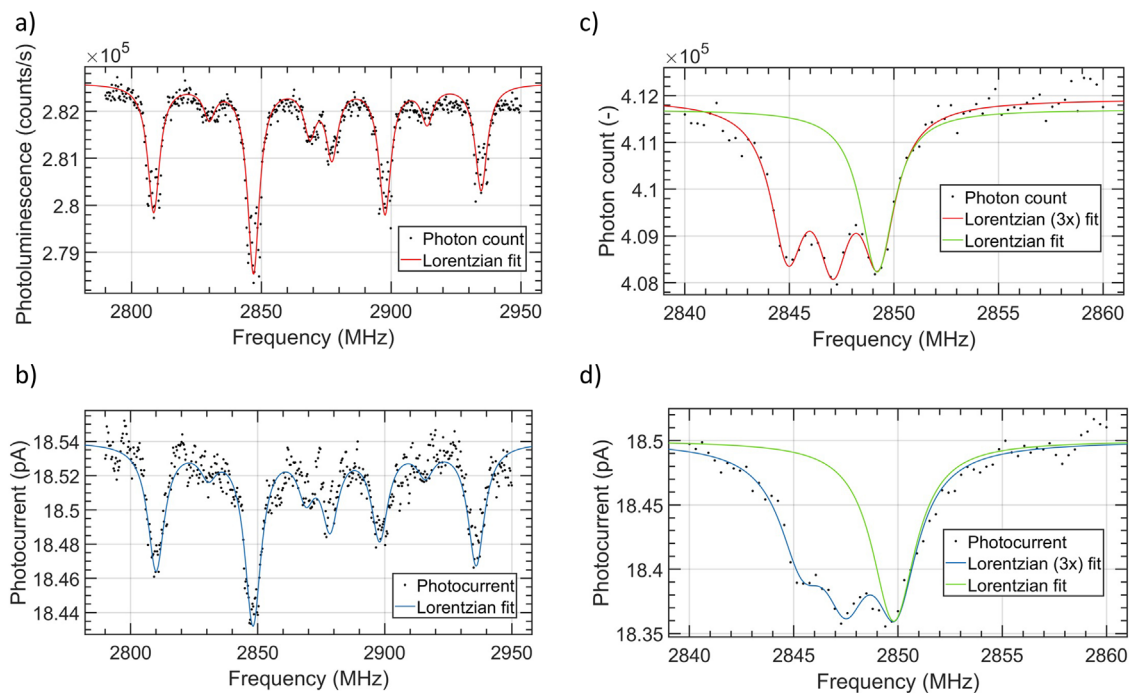


**FIG. 2.** The ODMR and PDMR spectra were measured using a yellow-green laser (561 nm). (a) ODMR and (b) PDMR spectra split into eight peaks using a permanent magnet. Single peak of the (c) ODMR and (d) PDMR spectra showing hyperfine interaction (FWHM = 1.95 MHz,  $C = 0.68\%$  and FWHM = 2.81 MHz,  $C = 0.87\%$ , respectively). Experimental conditions: laser power 2.4 mW, microwave power 20 mW, bias voltage +15 V. The fitting used for case (a) and (b) was eight peak Lorentzian fit, whereas in the case of (c) and (d), single and triple Lorentzian fitting was used.

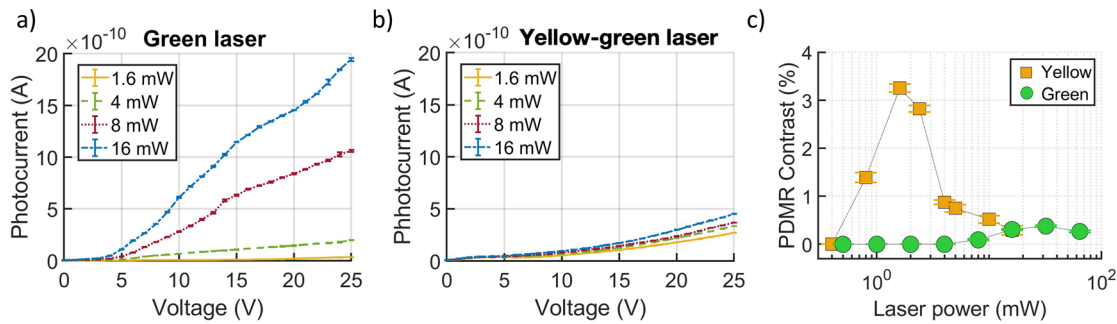


**FIG. 3.** Comparison of yellow-green and green laser illumination for photoelectric detection. (a) IV curve for green laser illumination measured with picoammeter. (b) IV curve for yellow-green laser illumination measured with picoammeter. (c) PDMR contrast as a function of laser excitation power. Microwave power 190 mW (for green), and 250 mW (for yellow-green), bias voltage +15 V.

the  $NV^0$  charge state to  $NV^-$  state.<sup>12,23</sup> The photon energy of the green laser (2.33 eV) is sufficient to ionize other diamond-related defects (such as P1 centers—photoionization onset  $\sim 2.25$  eV) resulting in higher detected photocurrent. On the other hand, using yellow-green (2.21 eV) illumination reduces the total photocurrent, which we attribute mainly to the reduction of P1 center photoionization, although some other defects can be involved as well.<sup>16</sup> Therefore, for the yellow-green excitation, we do not need to use very high laser power to have the two-photon NV photoionization dominate over the one-photon P1 center photoionization. Consequently, the yellow-green is more efficient for NV current generation in terms of the signal-to-background ratio.

Further on, we measured the PDMR and ODMR spectra in the range 2.7–3 GHz for both the yellow-green and the green laser excitations to examine the value of the spin contrast. We fit the measured resonance peaks (both for PL and photocurrent detection) using a Lorentzian function and calculated the magnetic resonance contrast from the fit. The resulting PDMR contrast dependence on the laser power and laser wavelength is depicted in Fig. 3(c). At lower laser powers (below  $\sim 5$  mW), a high spin contrast is observed for yellow-green light excitation, whereas we did not observe any spin contrast for the green. (In this case, the resonance is buried in the noise, as the NV photocurrent modulates the P1 photocurrent.) The maximal PDMR contrast obtained under yellow-green illumination ( $\sim 3.2\%$ ) is similar to the maximal ODMR contrast observed under the same excitation wavelength (see below) for the measured sample. This fact supports our conclusions about the lower probability of P1 center ionization by a 561 nm laser. At higher laser powers, the PDMR contrast is relatively low for both laser colors. We attribute this effect to the too high rate of light-induced spin polarization compared to the Rabi driving rate (proportional to the square root of the MW power) for high optical excitation powers, as well documented in the literature.<sup>24</sup> The best conditions, yielding the highest PDMR contrast for given MW power, were for yellow-green excitation at 1.6 mW. Notably, we observe that the spin contrast maximum is shifted to lower laser powers for yellow-green spin contrast maximum as compared to green photoionization. This fact is in line with enhanced generation of photocurrent from P1 centers using the green light. Also, we consume some photons for P1 photoionization (i.e., our effective optical power on the NV centers is lower); therefore, NV excitation rates for green are lower and the maximum contrast is obtained at higher laser powers as compared to yellow excitation.

Based on the experimental results, we predict the sensitivity for the PDMR magnetometry and compare it to the ODMR. For this purpose, we used the shot-noise limited sensitivity ( $\eta$ ) formula of the NV system<sup>25</sup>

$$\eta = \frac{4h}{3\sqrt{3}g\mu_B} \cdot \frac{\nu}{c\sqrt{R}}, \quad (2)$$

where  $h$  is the Planck constant,  $g$  is the NV gyromagnetic ratio,  $\mu_B$  is the Bohr magneton,  $c$  is the experimental spin contrast,  $\nu$  is the measured FWHM, and  $R$  is the signal (i.e., the number of detected photons per second for ODMR or electrons per second for PDMR).

The calculated sensitivities based on the measured data are shown in Fig. 4 together with the experimental values of FWHM, spin contrast, and the detection rate. The PDMR measurements with low power green excitation did not lead to any detectable contrast within the signal/noise ratio limits as discussed above. In the case of the yellow-green excitation, the spin contrast was significantly enhanced, equaling the contrast of ODMR for the same excitation wavelength. Because under low excitation power, the FWHM was also similar for both readout techniques, it is mainly the total photoelectric detection rate with respect to the photon count for ODMR that leads to the enhanced magnetic field sensitivity obtained using PDMR. Noticeably for both the green (for higher laser power) and the yellow-green illuminations (in all measured laser power range), PDMR leads to improved sensitivity compared to ODMR. It should be noted that thanks to the laser power dependent contrast discussed above, the use of yellow-green excitation enables to reach a high PDMR sensitivity under considerably reduced laser power. As mentioned earlier, we used low-density NV ensembles with a typical concentration around 10 ppb (200 NV centers in the volume contributing to the photoelectric signal). This corresponds to CW PDMR magnetic field sensitivity of about  $100 \text{ nT/Hz}^{1/2}$ , which compares approximately to  $\sim 1 \mu\text{T/Hz}^{1/2}$  for single NV CW ODMR sensitivity in the scanning nanoprobes.<sup>14</sup> The sample that we used for our experiment has rather broad resonance lines, with FWHM in the range of 10 MHz. By using hyperfine lines due to interaction with the  $^{14}\text{N}$  spin, the linewidth of about 3 MHz was achieved. However, the FWHM can be further reduced significantly (i.e., below 100 kHz) for low NV doped samples, for example, by using  $^{12}\text{C}$  isotopically enhanced diamond, thus improving the sensitivity to  $1 \text{ nT/Hz}^{1/2}$ . By increasing the NV concentration and the input laser power, the sensitivity could also be further enhanced significantly.

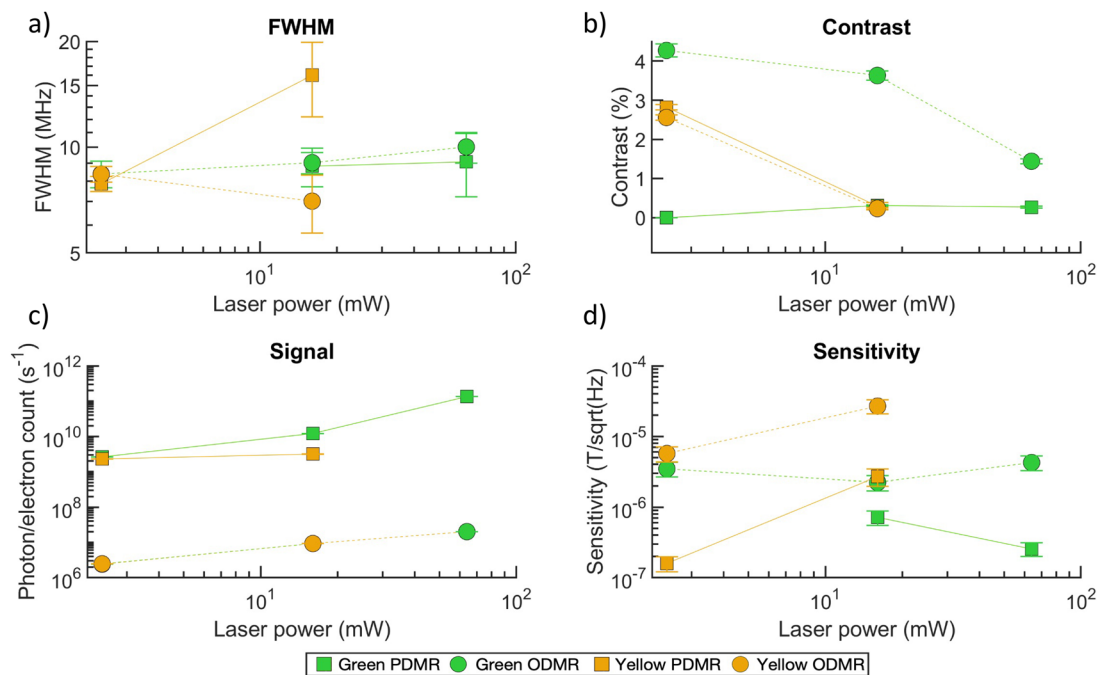


**FIG. 4.** Magnetic field sensitivity predictions for PDMR and ODMR using a yellow-green and green laser. (a) Effect of laser power on the FWHM and (b) on the measured spin contrast. (c) Effect of laser power on detection rate. (d) Sensitivity dependency on laser power. Gray lines serve for eye guidance. Microwave power 190 mW (for green), and 250 mW (for yellow-green). Bias voltage +15 V.

Optimization of the device geometry as well as using diamond with narrow NV resonance bandwidth will allow further improvement in the sensitivity. The advantages of our approach are demonstrated tenfold increased performance of PDMR compared to ODMR on the same low NV density sample and the possibility to use our method for devices that are fully integrable in compact magnetometers.

In summary, we have studied the sensitivity of the electrical readout technique for magnetometry measurement using a CVD-grown diamond sample with low NV concentration. We show that the selection of the laser excitation wavelength is of importance in order to achieve optimal magnetic field sensitivity. The PDMR performances obtained using a yellow-green (561 nm) laser surpass the performances of a green laser (532 nm); the higher wavelength illumination enables us to achieve a better signal-to-background ratio by suppressing the photoionization of defects other than NV centers (such as P1 centers). It consequently allows us to carry out the PDMR measurements at lower laser powers with increased magnetic resonance contrast. In comparison with ODMR, photoelectric readout leads to ten times improved shot noise limit of the magnetic field sensitivity in the selected conditions. Future experimental work is necessary to gain a better understanding of the possible charge exchanges between NV centers and other donor or acceptor defects in diamond, which could affect the PDMR contrast. For making the best use of the PDMR magnetometry in practical devices, the technical noise should be further reduced. Essential for this is designing low noise preamplifiers as well as reduction of microwave–photocurrent cross talks, which will be addressed in follow-up works.

M.N. acknowledges the QuantERA projects Q-Magine No. S010518N and NanoSpin No. S010418N, which are funded through the Flemish Scientific Foundation (FWO), as well as FWO Project Nos. G0E7417N and G0A0520N and Quantum Flagship ASTERIQS Project No. 820394 and DIAQUANT Project No. S004018N, funded by SBO-FWO. J.H. is a Ph.D. fellow of the FWO No. 11D6620N.

## AUTHOR DECLARATIONS

### Conflict of Interest

The authors have no conflicts to disclose.

### Author Contributions

J.H. conducted the measurements. M.G. and E.B. carried out experimental optimization of detection setup. J.H. developed acquisition software and tailored the setup for photocurrent magnetometry readout; he also fabricated electrodes on the diamond sample and was mentored by M.M., E.B., and M.N., and I.P.R. supervised partial sub-projects and took part in detailed discussion of results. M.V.P. performed the electron spin properties measurements. J.H., M.G., E.B., and M.N. contributed to the manuscript writing. All authors discussed the results and commented on the manuscript. M.N. supervised the joint efforts.

### DATA AVAILABILITY

The data that support the findings of this study are available from the corresponding author upon reasonable request.

## REFERENCES

- <sup>1</sup>T. Schönau, V. Zakosarenko, M. Schmelz *et al.*, “A three-axis SQUID-based absolute vector magnetometer,” *Rev. Sci. Instrum.* **86**(10), 105002 (2015).
- <sup>2</sup>Y. Sebbag, E. Talker, A. Naiman *et al.*, “Demonstration of an integrated nanophotonic chip-scale alkali vapor magnetometer using inverse design,” *Light Sci. Appl.* **10**(1), 54 (2021).
- <sup>3</sup>J. F. Barry, J. M. Schloss, E. Bauch *et al.*, “Sensitivity optimization for NV-diamond magnetometry,” *Rev. Mod. Phys.* **92**(1), 015004 (2020).
- <sup>4</sup>L. Rondin, J.-P. Tetienne, T. Hingant *et al.*, “Magnetometry with nitrogen-vacancy defects in diamond,” *Rep. Prog. Phys.* **77**(5), 056503 (2014).
- <sup>5</sup>F. M. Stürner, A. Brenneis, T. Buck *et al.*, “Integrated and portable magnetometer based on nitrogen-vacancy ensembles in diamond,” *Adv. Quantum Technol.* **4**(4), 2000111 (2021).
- <sup>6</sup>T. Wolf, P. Neumann, K. Nakamura *et al.*, “Subpicotesla diamond magnetometry,” *Phys. Rev. X* **5**(4), 041001 (2015).
- <sup>7</sup>F. M. Stürner, A. Brenneis, J. Kassel *et al.*, “Compact integrated magnetometer based on nitrogen-vacancy centres in diamond,” *Diamond Relat. Mater.* **93**, 59–65 (2019).
- <sup>8</sup>E. Bourgeois, A. Jarmola, P. Siyushev *et al.*, “Photoelectric detection of electron spin resonance of nitrogen-vacancy centres in diamond,” *Nat. Commun.* **6**(1), 8577 (2015).
- <sup>9</sup>E. Bourgeois, E. Londero, K. Buczak *et al.*, “Enhanced photoelectric detection of NV magnetic resonances in diamond under dual-beam excitation,” *Phys. Rev. B* **95**(4), 041402 (2017).
- <sup>10</sup>M. Gulka, E. Bourgeois, J. Hruba *et al.*, “Pulsed photoelectric coherent manipulation and detection of NV center spins in diamond,” *Phys. Rev. Appl.* **7**(4), 044032 (2017).
- <sup>11</sup>F. M. Hrubesch, G. Braunbeck, M. Stutzmann *et al.*, “Efficient electrical spin readout of NV centers in diamond,” *Phys. Rev. Lett.* **118**(3), 037601 (2017).
- <sup>12</sup>M. Gulka, D. Wirtitsch, V. Ivády *et al.*, “Room-temperature control and electrical readout of individual nitrogen-vacancy nuclear spins,” *Nat. Commun.* **12**(1), 4421 (2021).
- <sup>13</sup>T. Murooka, M. Shiigai, Y. Hironaka *et al.*, “Photoelectrical detection of nitrogen-vacancy centers by utilizing diamond lateral p–i–n diodes,” *Appl. Phys. Lett.* **118**(25), 253502 (2021).
- <sup>14</sup>M. S. Grinolds, S. Hong, P. Maletinsky *et al.*, “Nanoscale magnetic imaging of a single electron spin under ambient conditions,” *Nat. Phys.* **9**(4), 215–219 (2013).
- <sup>15</sup>D. L. Sage, K. Arai, D. R. Glenn *et al.*, “Optical magnetic imaging of living cells,” *Nature* **496**(7446), 486–489 (2013).
- <sup>16</sup>E. Bourgeois, M. Gulka, and M. Nesladek, “Photoelectric detection and quantum readout of nitrogen-vacancy center spin states in diamond,” *Adv. Opt. Mater.* **8**(12), 1902132 (2020).
- <sup>17</sup>M. Nesládek, K. Meykens, L. M. Stals *et al.*, “Origin of characteristic subgap optical absorption in CVD diamond films,” *Phys. Rev. B* **54**(8), 5552–5561 (1996).
- <sup>18</sup>W. J. P. van Enckevort and E. H. Versteegen, “Temperature dependence of optical absorption by the single-substitutional nitrogen donor in diamond,” *J. Phys.: Condens. Matter* **4**(9), 2361–2373 (1992).
- <sup>19</sup>M. Nesládek, L. M. Stals, A. Stesmans *et al.*, “Dominant defect levels in diamond thin films: A photocurrent and electron paramagnetic resonance study,” *Appl. Phys. Lett.* **72**(25), 3306–3308 (1998).
- <sup>20</sup>J. Rosa, M. Vaněček, M. Nesládek *et al.*, “On Photocurrent (and EPR) Study of Defect Levels in CVD Diamond,” *Phys. Status Solidi A* **172**(1), 113–122 (1999).
- <sup>21</sup>N. Aslam, G. Waldherr, P. Neumann *et al.*, “Photo-induced ionization dynamics of the nitrogen vacancy defect in diamond investigated by single-shot charge state detection,” *New J. Phys.* **15**(1), 013064 (2013).
- <sup>22</sup>L. Razinkovas, M. Maciaszek, F. Reinhard *et al.*, “Photoionization of negatively charged NV centers in diamond: Theory and ab initio calculations,” *Phys. Rev. B* **104**(23), 235301 (2021).
- <sup>23</sup>P. Siyushev, M. Nesladek, E. Bourgeois *et al.*, “Photoelectrical imaging and coherent spin-state readout of single nitrogen-vacancy centers in diamond,” *Science* **363**(6428), 728–731 (2019).
- <sup>24</sup>K. Jensen, V. M. Acosta, A. Jarmola *et al.*, “Light narrowing of magnetic resonances in ensembles of nitrogen-vacancy centers in diamond,” *Phys. Rev. B* **87**(1), 014115 (2013).
- <sup>25</sup>A. Dréau, M. Lesik, L. Rondin *et al.*, “Avoiding power broadening in optically detected magnetic resonance of single NV defects for enhanced dc magnetic field sensitivity,” *Phys. Rev. B* **84**(19), 195204 (2011).